# Article

# The contribution of insects to global forest deadwood decomposition

A list of authors and affiliations appears at the end of the paper.

The amount of carbon stored in deadwood is equivalent to about 8 per cent of the global forest carbon stocks[1]. The decomposition of deadwood is largely governed by climate[2–5] with decomposer groups—such as microorganisms and insects— contributing to variations in the decomposition rates[2,6,7]. At the global scale, the contribution of insects to the decomposition of deadwood and carbon release remains poorly understood[7]. Here we present a field experiment of wood decomposition across 55 forest sites and 6 continents. We find that the deadwood decomposition rates increase with temperature, and the strongest temperature effect is found at high precipitation levels. Precipitation affects the decomposition rates negatively at low temperatures and positively at high temperatures. As a net effect— including the direct consumption by insects and indirect effects through interactions with microorganisms—insects accelerate the decomposition in tropical forests (3.9% median mass loss per year). In temperate and boreal forests, we find weak positive and negative effects with a median mass loss of 0.9 per cent and −0.1 per cent per year, respectively. Furthermore, we apply the experimentally derived decomposition function to a global map of deadwood carbon synthesized from empirical and remote-sensing data, obtaining an estimate of 10.9 ± 3.2 petagram of carbon per year released from deadwood globally, with 93 per cent originating from tropical forests. Globally, the net effect of insects may account for 29 per cent of the carbon flux from deadwood, which suggests a functional importance of insects in the decomposition of deadwood and the carbon cycle.

The world's forests are an important carbon sink[1], but global climate change is affecting carbon sequestration and release by altering tree growth[8,9], mortality[10,11] and decomposition[12,13]. Therefore, a comprehensive understanding of the forest carbon cycle and its climate sensitivity is critical for improving global climate change projections. Whereas previous research has focused strongly on carbon sequestration[14,15], the release of carbon—including through the decomposition of deadwood—remains poorly understood[7,16]. Deadwood currently stores 73 ± 6 petagram (Pg; 10[15] g) of carbon (C) globally, which is about 8% of the global forest carbon stock[1] and 8.5% of atmospheric carbon[17]. The decomposition of deadwood is largely governed by climate[2–5], with the activity of different decomposer groups contributing to the considerable variation in decomposition rates[2,6,7]. Recently, the role of fungi in forest carbon cycling has received much attention[2,6] and they are believed to be the principal decomposers of deadwood[5–7]. Although local- and regional-scale studies indicate that insects can also make a considerable contribution to wood decomposition[7], global assessments that quantify the role of microorganisms and insects are lacking. Given the sensitivity of insects to climate change[18,19] and the observed declines in insect biodiversity[20–22], a better understanding of the interactions between insect decomposers and climate is needed to more robustly project carbon flux from deadwood and the role of deadwood in the global forest carbon sink[11,16,23].

Here we quantified the role of deadwood-decomposing insects relative to climate by conducting standardized field experiments of wood decomposition across 55 sites on six continents (Fig. 1a). Our sites were selected to capture the gradient of temperature and precipitation conditions under which forests occur globally. Insects and other animals (hereafter collectively termed insects for brevity) had unrestricted access to wood placed on the forest floor in the uncaged treatment in our experiment, whereas they were excluded from the wood in the closed-cage treatment using mesh cages (Extended Data Fig. 1). Our estimate of the effect of insects on wood decomposition was quantified as the difference between the decomposition rates in the uncaged and closed-cage treatments. This measure can be considered the 'net effect of insects', consisting of the direct consumption of wood by insects and indirect effects through interactions with microorganisms. The latter effects include—for example—competition for resources, grazing on fungal mycelia, creation of entry ports or vectoring, and these can therefore either increase[24] or decrease wood decomposition[25,26]. As a consequence, the direct consumption by insects could be higher than our net estimate at sites where the interactions between insects and microorganisms decrease the decomposition rates. To explore the effects of caging on microclimatic conditions and decomposition rates, we implemented a third treatment (open cage) using cages with holes, which allow insects access to the wood samples under similar microclimatic conditions to those logs in the closed-cage treatment (Supplementary Information section 1). We assessed deadwood decomposition as the loss of dry mass over a period of up to 3 years for wood samples with bark (around 3 cm in diameter, 50 cm in length) of locally dominant native tree species (142 tree species in total) as well as for standardized wooden dowels without bark. In total, we recorded wood mass loss for 4,437 individual samples. We used a Gaussian generalized linear mixed log-link model with site-specific random effects to quantify the

# Article

influence of insects (uncaged versus closed cages), site-level temperature and precipitation as well as the type of wood (angiosperm versus gymnosperm) on the annual rates of wood mass loss. Although some influence of caging on microclimate cannot be ruled out, we focused on the comparison between uncaged and closed-cage treatments, because analyses across treatments indicated that this comparison provides the most robust estimate for the net effect of insects on wood decomposition (Supplementary Information section 1, Extended Data Table 1 and Extended Data Fig. 2).

To provide an estimate of the global carbon flux from deadwood decomposition (hereafter referred to as deadwood carbon release) and to quantify the functional importance of insects for global deadwood carbon, we applied the model derived from our decomposition experiment to a new global deadwood carbon map (Fig. 1a), which we synthesized from empirical and remote-sensing data. As the global modelling of deadwood remains challenging, we conducted in-depth analyses of uncertainty, evaluating the decomposition function derived from our experiment against independent empirical data[27] and quantifying the relative contribution of different sources of uncertainty in a sensitivity analysis (Supplementary Information section 2 and Extended Data Table 2). The sensitivity analysis also highlights how further research can improve the modelling of global carbon fluxes from deadwood.

## Climate and insect effects

In our global experiment, the wood decomposition rate was the highest in the tropics/subtropics (hereafter called tropics; median = 28.2% mass loss per year), and was considerably lower in the temperate (median = 6.3%) and boreal/hemiboreal (hereafter called boreal; median = 3.3%) biomes (Fig. 1b). Wood decomposition rates were highly climate-sensitive, driven by the complex interplay between temperature and precipitation (Table 1). Decomposition rates increased with increasing temperature across the full gradient of precipitation, but the effects of temperature were strongest at high levels of precipitation (Fig. 2a and Extended Data Fig. 3a). Precipitation affected decomposition rates negatively at low temperatures but positively at high temperatures. The observed positive global relationship between wood decomposition and temperature was similar to patterns observed at local-to-continental scales[2,4], as well as for the decomposition of non-woody litter[12,28], and is consistent with general theory, which predicts an increase in metabolic rates and enzymatic activity with temperature[29]. Moreover, the length of the vegetation period usually increases with temperature, which may further increase annual decomposition rates. Weaker positive effects of temperature on wood decomposition under low levels of precipitation may be the result of low levels of moisture in the wood, limiting microbial activity[30,31] and selecting for drought-tolerant fungal species that have a reduced ability to decompose wood[6]. Given that temperature is predicted to increase globally[32], our results indicate that wood decomposition rates are likely to increase in the future. The strength of this increase will be modulated by current and future levels of precipitation and the emerging water balance of a site[33]. Decomposition rates were higher for angiosperms than for gymnosperms (Table 1), which is consistent with results from a global meta-analysis and can be explained by differences in wood traits[34]. Results for standardized wooden dowels were similar to those of wood from native tree species (Extended Data Table 1).

Insect access to deadwood affected decomposition, but this effect was contingent on climatic conditions (Table 1). The net effect of insects on decomposition was particularly high in the tropics (median = 3.9% mass loss per year) (Fig. 1c). By contrast, effects were low in the temperate biome and even negative in the boreal biome (median of 0.9% and −0.1%, respectively) (Fig. 1c). The net effect of insects generally increased with temperature, with effect size strongly mediated by precipitation (Table 1). At low levels of precipitation, temperature had only a minor influence on the net effect of insects. By contrast,
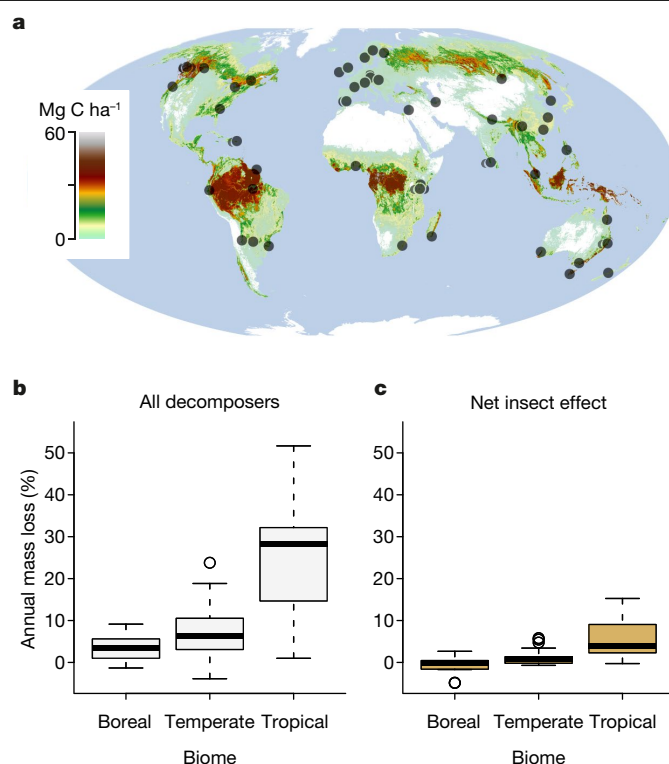


**Fig. 1 | Decomposition rates and insect effects per biome. a**, Estimated carbon pools in deadwood with a diameter of >2 cm (Mg C ha⁻¹) with 5 arcmin spatial resolution and the location of the 55 experimental sites (grey dots). **b**, **c**, Annual mass loss of deadwood of native tree species when all decomposer groups have access (uncaged treatment) (**b**) and the difference in annual mass loss between uncaged and closed-cage treatments that are attributed to the net effect of insects (**c**). Data are predicted values for both angiosperm and gymnosperm species at 55 and 21 sites, respectively, based on a Gaussian generalized linear mixed log-link model for 2,533 logs with site-specific random effects and temperature, precipitation, treatment and host type, as well as their interactions, as fixed effects (Table 1). Boxes represent data within the 25th and 75th percentile, black lines show the medians and whiskers extend to 1.5× the interquartile range. Note that the classification into biomes is shown for illustrative purposes, whereas the statistical model is based on continuous climate variables.

at high levels of precipitation, temperature was a strong driver of the net effect of insects on decomposition (Fig. 2b and Extended Data Fig. 3b). At high temperatures, increasing precipitation increased the net effect of insects, whereas at low temperatures, increasing precipitation resulted in a negative net effect of insects. Thus, decomposition rates were higher when insects were excluded at low temperatures and high precipitation. The complex relationships between insects and climate are driving several mechanisms that determine the net effect of insects on wood decomposition. First, wood-feeding termites are a key group of decomposers[7,35], but are largely restricted to regions with high temperatures (Fig. 2b). Nevertheless, considerable variation in the net effect of insects also exists among sites at which termites are present (Fig. 2b), underlining the importance of factors in addition to termite occurrence. Second, temperature affects the metabolic rate of insects, increasing consumption and accelerating larval development directly[18] as well as indirectly through enhanced food quality[36]. Third, insects can be negatively affected by high wood moisture when precipitation is high and evaporation low, as is the case in humid boreal forests, for example (Extended Data Fig. 3b), due to low aeration or high pathogen pressure[37]. Conversely, moisture is a limiting factor at high temperatures, restricting the period of high insect activity to the rainy season[38]. Fourth, interactions between insects and microorganisms can

**Table 1 | Drivers of wood decomposition**

| Predictor | Estimate (×10³) | s.e. (×10³) | z value | P value | Relative effect and 95% CI |
|---|---|---|---|---|---|
| Temperature (°C) | −11.009 | 3.021 | −3.644 | <0.001 | 0.989 (0.983–0.995) |
| Precipitation (dm yr⁻¹) | −3.135 | 3.322 | −0.944 | 0.345 | 0.997 (0.990–1.003) |
| Host: angiosperm | −150.477 | 22.506 | −6.686 | <0.001 | 0.860 (0.823–0.899) |
| Host: gymnosperm | −82.825 | 24.862 | −3.331 | 0.001 | 0.921 (0.877–0.966) |
| Treatment: uncaged versus closed | −29.228 | 5.694 | −5.133 | <0.001 | 0.971 (0.960–0.982) |
| Temperature×precipitation | −0.565 | 0.401 | −1.408 | 0.159 | 0.999 (0.999–1.000) |
| Temperature×host | 5.016 | 1.250 | 4.014 | <0.001 | 1.005 (1.003–1.007) |
| Precipitation×host | −0.434 | 3.587 | −0.121 | 0.904 | 1.000 (0.993–1.007) |
| Temperature×treatment | −4.161 | 0.742 | −5.608 | <0.001 | 0.996 (0.994–0.997) |
| Precipitation×treatment | −5.236 | 0.923 | −5.675 | <0.001 | 0.995 (0.993–0.997) |
| Temperature×precipitation×host | 0.104 | 0.327 | 0.317 | 0.751 | 1.000 (0.999–1.001) |
| Temperature×precipitation×treatment | −0.728 | 0.113 | −6.451 | <0.001 | 0.999 (0.999–0.999) |

Results from a Gaussian generalized linear mixed log-link model of the relative annual mass loss of wood of native tree species derived from a global deadwood decomposition experiment. The model is based on data from closed-cage and uncaged treatments, comprising 2,533 logs of native tree species from 55 sites. Fixed effects were the mean annual temperature and the mean annual precipitation, which were both centred and scaled, host tree type (angiosperm versus gymnosperm) and treatment, as well as their two- and three-way interactions, with site as a random effect. Estimates and standard errors of the maximum likelihood estimates (s.e.) for temperature and precipitation are transformed back to °C and dm yr⁻¹, respectively. The main effects for each variable are interpretable when the remaining variables are fixed to their reference value (15 °C and 13 dm yr⁻¹). A relative effect (that is, the exp(estimate)) of, for instance, 0.989 indicates that for a temperature increase of 1 °C with all other variables fixed (precipitation at 13 dm yr⁻¹, host and treatment), the deadwood dry mass after 1 year would be 98.9% of the mass without this change in temperature. This represents an additional mass loss of 1.1% induced by a 1 °C increase in temperature. The marginal $R^2$ of the model was 0.84.

decrease wood decomposition: insects, for example, can introduce fungal species that do not contribute strongly to wood decomposition themselves, while suppressing other principal wood-decomposing fungi, thus lowering the overall decomposition rate[25]. In cold and humid regions, such biotic interactions could outweigh the effects of direct consumption and lead to an overall negative net effect of insects on wood decomposition.

Our findings indicate that wood decomposition is driven by a complex interplay of temperature and precipitation with the decomposer community. Climate warming could accelerate wood decomposition by increasing microbial activity and insect-mediated wood decomposition, particularly in regions in which moisture is not limiting. However, increased drying as a result of global climate change could also decrease the decomposition of deadwood. Our results support that biodiversity loss of insects has the potential to affect deadwood decomposition, but that effects may vary regionally. To improve predictions of the functional effects of biodiversity loss, more research is needed on how specific components of decomposer communities (that is, biomass, species number, functional composition and species interactions) influence deadwood decomposition[7]. Our work suggests that the strongest functional effects of changes in the decomposer community will occur in regions with a warm and humid climate, which should be a particular focus of further research.

## Global carbon flux estimate

To assess the role of deadwood decomposition in the global carbon cycle, we applied the relationship between decomposition rates and local climate derived from our global experiment (Table 1) to a map of the global carbon currently stored in deadwood (Fig. 1a). As our experiment focused on small-diameter deadwood over 3 years, we adjusted the decomposition rates to account for slower mass loss of large-diameter deadwood (details are provided in the Methods and Supplementary Information section 2). We evaluated our relationship between decomposition rate and local climate against 157 independent empirical observations from previous deadwood surveys[27], spanning the full range of deadwood diameters of >7 cm, time since tree death and climatic conditions. We obtained a good match between the results from our model and these independent data (Extended Data Fig. 4), suggesting that our approach is robust.

We estimate that 10.9 ± 3.2 Pg C could be released from deadwood per year globally. This suggests that the decomposition of deadwood could be an important flux in the global carbon cycle. Our estimate
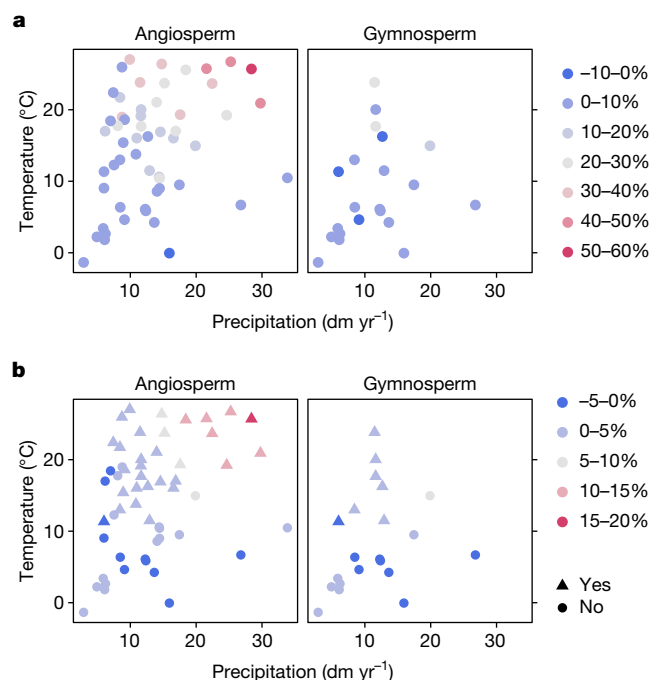
**Fig. 2 | Decomposition rates and net insect effects in climate space.** a, b, Annual mass loss of deadwood of native tree species, considering all possible groups of decomposers (uncaged treatment) (a) and annual mass loss attributed to insects (difference in mass loss between uncaged and closed-cage treatments), b, relative to the mean annual temperature and mean annual precipitation. Symbols indicate whether termites occur in the study areas. Points represent predicted values for angiosperm species at 55 sites and gymnosperm species at 21 sites based on a Gaussian generalized linear mixed log-link model for 2,533 logs with site-specific random effects and temperature, precipitation, treatment, host division, as well as their interactions, as fixed effects. Note that the lower sample size for gymnosperm species represents their global distribution.
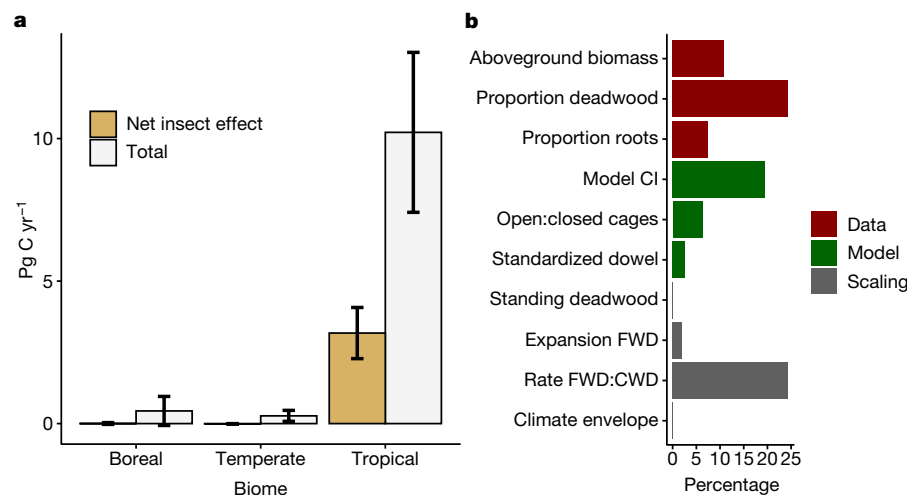
# Article



**Fig. 3 | Global annual carbon release from deadwood and sensitivity analysis. a**, Annual carbon released (Pg C yr⁻¹) from deadwood per biome. Error bars indicate the uncertainty of the biome-specific estimate as determined by the sensitivity analysis. **b**, Relative contributions to the overall uncertainty of the global estimate of total carbon release from the decomposition of deadwood. The colour of the bars indicates the uncertainty category. CI, confidence interval; CWD, coarse wood debris; FWD, fine woody debris. See Extended Data Table 2 for a detailed description of each factor and an uncertainty assessment of the net insect effect.

corresponds to 15–25% of the annual release of carbon from soils globally (estimated to be 50–75 Pg C yr⁻¹ (ref. [28])) and is 115% of the current anthropogenic carbon emissions from fossil fuels (9.5 Pg C yr⁻¹ (ref. [17])). We note, however, that not all carbon that is released from deadwood through decomposition is emitted to the atmosphere, as parts are immobilized in the biosphere or in soils[39,40]. Carbon release from deadwood is highest in tropical biomes (10.2 Pg C yr⁻¹) (Fig. 3a and Extended Data Table 3), where large deadwood carbon pools and high decomposition rates coincide (Extended Data Fig. 5). Although deadwood carbon stocks are also considerable in temperate and boreal biomes (amounting to 35% of all carbon stored in deadwood globally), the climatic limitations for wood decomposition as well as differences in decomposer communities (for example, the absence of termites) render annual carbon fluxes from deadwood much smaller in these biomes (that is, 0.44 Pg C yr⁻¹ and 0.28 Pg C yr⁻¹ in boreal and temperate forests, respectively), accounting for less than 7% of the global carbon release from deadwood. Globally, the net effect of insects on wood decomposition may result in a carbon flux of 3.2 ± 0.9 Pg C yr⁻¹, which represents 29% of the total carbon released from deadwood (Fig. 3a and Extended Data Fig. 5).

Our global estimates are only a first step to a better quantification of the role of deadwood decomposition in the global carbon cycle. Uncertainties related to the underlying data, the statistical models and other assumptions necessary for upscaling our experimental results were assessed in a global sensitivity analysis. This analysis bounded the uncertainty of global annual carbon release from deadwood and the net effect of insects at approximately ±25% around the mean. Of the various sources of uncertainty that were considered, the underlying data on deadwood carbon stocks contributed most strongly to the overall uncertainty (Fig. 3, Extended Data Table 2 and Supplementary Information section 2). Our results suggest that assessments of the global deadwood carbon cycle could be improved by more accurately quantifying deadwood stocks in tropical forests. Although the effects of wildfire were included in our deadwood carbon map through the underlying inventory data, we did not explicitly consider deadwood carbon release from fire. We note, however, that a large portion of the carbon stored in deadwood is not combusted in wildfires[41,42]. Further uncertainty results from our experimental design included the following. It cannot be ruled out that altered microclimatic conditions in cages affected the estimates of the net effect of insects derived from the comparison between closed-cage and uncaged treatments. Such a bias would lead to an underestimation of the net insect effect in the tropics and an overestimation in the temperate zone (Supplementary Information section 1). When the global annual net effect of insects on deadwood decomposition was derived from the comparison of closed-cage and open-cage treatments, it still amounted to 1.76 Pg C.

However, this value underestimates the true effect of insects due to a reduction in insect colonization in the open-cage treatment (Extended Data Fig. 2 and Supplementary Information section 1).

Our experiment highlights that deadwood and wood-decomposing insects have an important role in the global carbon cycle. In contrast to the prevailing paradigm that insects generally accelerate wood decomposition[7], our results indicate that their functional role is more variable, and is contingent on the prevailing climatic conditions. We conclude that ongoing climate warming[32] will likely accelerate decomposition by enhancing the activity of microorganisms and insects—an effect that will be particularly strong in regions in which moisture is not limiting. To robustly project the future of the forest carbon sink[23,43], dynamic global vegetation models need to account for the intricacies of both deadwood creation (for example, through natural disturbances) and deadwood decomposition.

## Online content

Any methods, additional references, Nature Research reporting summaries, source data, extended data, supplementary information, acknowledgements, peer review information; details of author contributions and competing interests; and statements of data and code availability are available at https://doi.org/10.1038/s41586-021-03740-8.

1. Pan, Y. et al. A large and persistent carbon sink in the world's forests. *Science* **333**, 988–993 (2011).
2. Bradford, M. A. et al. Climate fails to predict wood decomposition at regional scales. *Nat. Clim. Change* **4**, 625–630 (2014).
3. Chambers, J. Q., Higuchi, N., Schimel, J. P. J., Ferreira, L. V. & Melack, J. M. Decomposition and carbon cycling of dead trees in tropical forests of the central Amazon. *Oecologia* **122**, 380–388 (2000).
4. González, G. et al. Decay of aspen (*Populus tremuloides* Michx.) wood in moist and dry boreal, temperate, and tropical forest fragments. *Ambio* **37**, 588–597 (2008).
5. Stokland, J., Siitonen, J. & Jonsson, B. G. *Biodiversity in Dead Wood* (Cambridge Univ. Press, 2012).
6. Lustenhouwer, N. et al. A trait-based understanding of wood decomposition by fungi. *Proc. Natl Acad. Sci. USA* **117**, 11551–11558 (2020).
7. Ulyshen, M. D. Wood decomposition as influenced by invertebrates. *Biol. Rev. Camb. Philos. Soc.* **91**, 70–85 (2016).
8. Pretzsch, H., Biber, P., Schütze, G., Uhl, E. & Rötzer, T. Forest stand growth dynamics in Central Europe have accelerated since 1870. *Nat. Commun.* **5**, 4967 (2014).
9. Büntgen, U. et al. Limited capacity of tree growth to mitigate the global greenhouse effect under predicted warming. *Nat. Commun.* **10**, 2171 (2019).
10. Seidl, R. et al. Forest disturbances under climate change. *Nat. Clim. Change* **7**, 395–402 (2017).
11. Hubau, W. et al. Asynchronous carbon sink saturation in African and Amazonian tropical forests. *Nature* **579**, 80–87 (2020).
12. Portillo-Estrada, M. et al. Climatic controls on leaf litter decomposition across European forests and grasslands revealed by reciprocal litter transplantation experiments. *Biogeosciences* **13**, 1621–1633 (2016).
13. Christenson, L. et al. Winter climate change influences on soil faunal distribution and abundance: implications for decomposition in the northern forest. *Northeast. Nat.* **24**, B209–B234 (2017).

14. Keenan, T. F. et al. Increase in forest water-use efficiency as atmospheric carbon dioxide concentrations rise. *Nature* **499**, 324–327 (2013).

15. Stephenson, N. L. et al. Rate of tree carbon accumulation increases continuously with tree size. *Nature* **507**, 90–93 (2014).

16. Martin, A., Dimke, G., Doraisami, M. & Thomas, S. Carbon fractions in the world's dead wood. *Nat. Commun.* **12**, 889 (2021).

17. Friedlingstein, P. et al. Global carbon budget 2019. *Earth Syst. Sci. Data* **11**, 1783–1838 (2019).

18. Marshall, D. J., Pettersen, A. K., Bode, M. & White, C. R. Developmental cost theory predicts thermal environment and vulnerability to global warming. *Nat. Ecol. Evol.* **4**, 406–411 (2020).

19. Buczkowski, G. & Bertelsmeier, C. Invasive termites in a changing climate: a global perspective. *Ecol. Evol.* **7**, 974–985 (2017).

20. Diaz, S., Settele, J. & Brondizio, E. *Summary for Policymakers of the Global Assessment Report on Biodiversity and Ecosystem Services of the Intergovermental Science-Policy Platform on Biodiversity and Ecosystem Services* (IPBES, 2019).

21. van Klink, R. et al. Meta-analysis reveals declines in terrestrial but increases in freshwater insect abundances. *Science* **368**, 417–420 (2020).

22. Seibold, S. et al. Arthropod decline in grasslands and forests is associated with landscape-level drivers. *Nature* **574**, 671–674 (2019).

23. Harris, N. L. et al. Global maps of twenty-first century forest carbon fluxes. *Nat. Clim. Change* **11**, 234–240 (2021).

24. Jacobsen, R. M., Sverdrup-Thygeson, A., Kauserud, H., Mundra, S. & Birkemoe, T. Exclusion of invertebrates influences saprotrophic fungal community and wood decay rate in an experimental field study. *Funct. Ecol.* **32**, 2571–2582 (2018).

25. Skelton, J. et al. Fungal symbionts of bark and ambrosia beetles can suppress decomposition of pine sapwood by competing with wood-decay fungi. *Fungal Ecol.* **45**, 100926 (2020).

26. Wu, D., Seibold, S., Ruan, Z., Weng, C. & Yu, M. Island size affects wood decomposition by changing decomposer distribution. *Ecography* **44**, 456–468 (2021).

27. Harmon, M. E. et al. Release of coarse woody detritus-related carbon: a synthesis across forest biomes. *Carbon Balance Manag.* **15**, 1 (2020).

28. Wall, D. H. et al. Global decomposition experiment shows soil animal impacts on decomposition are climate-dependent. *Glob. Change Biol.* **14**, 2661–2677 (2008).

29. Gillooly, J. F., Brown, J. H., West, G. B., Savage, V. M. & Charnov, E. L. Effects of size and temperature on metabolic rate. *Science* **293**, 2248–2251 (2001).

30. Baldrian, P. et al. Responses of the extracellular enzyme activities in hardwood forest to soil temperature and seasonality and the potential effects of climate change. *Soil Biol. Biochem.* **56**, 60–68 (2013).

31. A'Bear, A. D., Jones, T. H., Kandeler, E. & Boddy, L. Interactive effects of temperature and soil moisture on fungal-mediated wood decomposition and extracellular enzyme activity. *Soil Biol. Biochem.* **70**, 151–158 (2014).

32. IPCC. *Climate Change 2014: Synthesis Report. Contribution of Working Groups I, II and III to the Fifth Assessment Report of the Intergovernmental Panel on Climate Change.* (IPCC, 2014).

33. Smyth, C. E., Kurz, W. A., Trofymow, J. A. & CIDET Working Group. Including the effects of water stress on decomposition in the Carbon Budget Model of the Canadian Forest Sector CBM-CFS3. *Ecol. Modell.* **222**, 1080–1091 (2011).

34. Weedon, J. T. et al. Global meta-analysis of wood decomposition rates: a role for trait variation among tree species? *Ecol. Lett.* **12**, 45–56 (2009).

35. Griffiths, H. M., Ashton, L. A., Evans, T. A., Parr, C. L. & Eggleton, P. Termites can decompose more than half of deadwood in tropical rainforest. *Curr. Biol.* **29**, R118–R119 (2019).

36. Birkemoe, T., Jacobsen, R. M., Sverdrup-Thygeson, A. & Biedermann, P. H. W. in *Saproxylic Insects* (ed. Ulyshen, M. D.) 377–427 (Springer, 2018).

37. Harvell, M. C. E. et al. Climate warming and disease risks for terrestrial and marine biota. *Science* **296**, 2158–2162 (2002).

38. Berkov, A. in *Saproxylic Insects* (ed. Ulyshen, M. D.) 547–580 (Springer, 2018).

39. Wang, C., Bond-Lamberty, B. & Gower, S. T. Environmental controls on carbon dioxide flux from black spruce coarse woody debris. *Oecologia* **132**, 374–381 (2002).

40. Peršoh, D. & Borken, W. Impact of woody debris of different tree species on the microbial activity and community of an underlying organic horizon. *Soil Biol. Biochem.* **115**, 516–525 (2017).

41. Campbell, J., Donato, D., Azuma, D. & Law, B. Pyrogenic carbon emission from a large wildfire in Oregon, United States. *J. Geophys. Res.* **112**, G04014 (2007).

42. van Leeuwen, T. T. et al. Biomass burning fuel consumption rates: a field measurement database. *Biogeosciences* **11**, 7305–7329 (2014).

43. McDowell, N. G. et al. Pervasive shifts in forest dynamics in a changing world. *Science* **368**, eaaz9463 (2020).

Sebastian Seibold[1,2,5,68 ✉], Werner Rammer[1], Torsten Hothorn[3], Rupert Seidl[1,2], Michael D. Ulyshen[4], Janina Lorz[5], Marc W. Cadotte[6], David B. Lindenmayer[7], Yagya P. Adhikari[8,9], Roxana Aragón[10], Soyeon Bae[11], Petr Baldrian[12], Hassan Barimani Varandi[13], Jos Barlow[14,15], Claus Bässler[16,17], Jacques Beauchêne[18], Erika Berenguer[14,19], Rodrigo S. Bergamin[20], Tone Birkemoe[21], Gergely Boros[22,23], Roland Brandl[24], Hervé Brustel[25], Philip J. Burton[26], Yvonne T. Cakpo-Tossou[27], Jorge Castro[28], Eugénie Cateau[25,29], Tyler P. Cobb[30], Nina Farwig[31], Romina D. Fernández[10], Jennifer Firn[32,33], Kee Seng Gan[34], Grizelle González[35], Martin M. Gossner[36], Jan C. Habel[37], Christian Hébert[38], Christoph Heibl[17], Osmo Heikkala[39], Andreas Hemp[40], Claudia Hemp[40], Joakim Hjältén[41], Stefan Hotes[42], Jari Kouki[43], Thibault Lachat[36,44], Jie Liu[45], Yu Liu[46], Ya-Huang Luo[45], Damasa M. Macandog[47], Pablo E. Martina[48],

Sharif A. Mukul[49], Baatarbileg Nachin[50], Kurtis Nisbet[51], John O'Halloran[52], Anne Oxbrough[53], Jeev Nath Pandey[54], Tomáš Pavlíček[55], Stephen M. Pawson[56,57], Jacques S. Rakotondranary[58,59], Jean-Baptiste Ramanamanjato[60], Liana Rossi[61], Jürgen Schmidl[62], Mark Schulze[63], Stephen Seaton[64], Marisa J. Stone[65], Nigel E. Stork[65], Byambagerel Suran[50], Anne Sverdrup-Thygeson[21], Simon Thorn[5], Ganesh Thyagarajan[66], Timothy J. Wardlaw[67], Wolfgang W. Weisser[68], Sungsoo Yoon[69], Naili Zhang[70] & Jörg Müller[5,17]

[1]Ecosystem Dynamics and Forest Management Group, School of Life Sciences, Technical University of Munich, Freising, Germany. [2]Berchtesgaden National Park, Berchtesgaden, Germany. [3]Epidemiology, Biostatistics and Prevention Institute, University of Zurich, Zurich, Switzerland. [4]Southern Research Station, USDA Forest Service, Athens, GA, USA. [5]Field Station Fabrikschleichach, University of Würzburg, Rauhenebrach, Germany. [6]Biological Sciences, University of Toronto Scarborough, Toronto, Ontario, Canada. [7]Fenner School of Environment and Society, The Australian National University, Canberra, Australian Capital Territory, Australia. [8]Department of Biogeography, University of Bayreuth, Bayreuth, Germany. [9]Department of Disturbance Ecology, University of Bayreuth, Bayreuth, Germany. [10]Instituto de Ecología Regional, CONICET-Universidad Nacional de Tucumán, Yerba Buena, Argentina. [11]Department of Animal Ecology and Tropical Biology, University of Würzburg, Würzburg, Germany. [12]Laboratory of Environmental Microbiology, Institute of Microbiology, The Czech Academy of Sciences, Prague, Czech Republic. [13]Agricultural and Natural Resources Research Centre of Mazandaran, Sari, Iran. [14]Lancaster Environment Centre, Lancaster University, Lancaster, UK. [15]Universidade Federal de Lavras, Lavras, Brazil. [16]Department of Biodiversity Conservation, Goethe-University Frankfurt, Frankfurt, Germany. [17]Bavarian Forest National Park, Grafenau, Germany. [18]CIRAD, UMR Ecologie des Forêts de Guyane (EcoFoG), AgroParisTech, CNRS, INRA, Universite des Antilles, Universite de Guyane, Kourou, France. [19]Environmental Change Institute, University of Oxford, Oxford, UK. [20]Grassland Vegetation Lab, Federal University of Rio Grande do Sul, Porto Alegre, Brazil. [21]Faculty of Environmental Sciences and Natural Resource Management, Norwegian University of Life Sciences, Aas, Norway. [22]Institute of Ecology and Botany, Centre for Ecological Research, Vácrátót, Hungary. [23] Institute for Wildlife Management and Nature Conservation, Hungarian University of Agriculture and Life Sciences, Gödöllő, Hungary. [24]Animal Ecology, University of Marburg, Marburg, Germany. [25]École d'Ingénieurs de Purpan, Université de Toulouse, UMR 1201 Dynafor, Toulouse, France. [26]Ecosystem Science and Management Program, University of Northern British Columbia, Terrace, British Columbia, Canada. [27]Laboratory of Applied Ecology, University of Abomey-Calavi, Godomey, Benin. [28]Department of Ecology, University of Granada, Granada, Spain. [29]Réserves Naturelles de France, Dijon, France. [30]Royal Alberta Museum, Edmonton, Alberta, Canada. [31]Conservation Ecology, University of Marburg, Marburg, Germany. [32]Science and Engineering Faculty, Queensland University of Technology, Brisbane, Queensland, Australia. [33]Centre for the Environment, Institute for Future Environments, Brisbane, Queensland, Australia. [34]Forest Research Institute Malaysia, Kuala Lumpur, Malaysia. [35]International Institute of Tropical Forestry, USDA Forest Service, San Juan, PR, USA. [36] Forest Entomology, Swiss Federal Research Institute WSL, Birmensdorf, Switzerland. [37]Evolutionary Zoology, University of Salzburg, Salzburg, Austria. [38]Natural Resources Canada, Canadian Forest Service, Quebec, Quebec, Canada. [39]Eurofins Ahma Oy, Oulu, Finland. [40]Department of Plant Systematics, University of Bayreuth, Bayreuth, Germany. [41]Department of Wildlife, Fish and Environmental Studies, Swedish University of Agricultural Sciences, Umeå, Sweden. [42]Applied Landscape Ecology, Chuo University, Tokyo, Japan. [43]School of Forest Sciences, University of Eastern Finland, Joensuu, Finland. [44]School of Agricultural, Forest and Food Sciences, Bern University of Applied Sciences, Zollikofen, Switzerland. [45]CAS Key Laboratory for Plant Diversity and Biogeography of East Asia, Kunming Institute of Botany, Chinese Academy of Sciences, Kunming, China. [46]ECNU-Alberta Joint Lab for Biodiversity Study, Tiantong National Station for Forest Ecosystem Research, East China Normal University, Shanghai, China. [47]Institute of Biological Sciences, University of the Philippines Los Banos, Laguna, The Philippines. [48]Department of Thermodynamics, Universidad Nacional del Nordeste, Resistencia, Argentina. [49]Tropical Forests and People Research Centre, University of the Sunshine Coast, Maroochydore, Queensland, Australia. [50]Forest Ecosystem Monitoring Laboratory, National University of Mongolia, Ulaanbaatar, Mongolia. [51]School of Environment and Science, Griffith University, Nathan, Queensland, Australia. [52]School of Biological, Earth and Environmental Sciences, University College Cork, Cork, Ireland. [53]Edge Hill University, Ormskirk, UK. [54]Institute of Forestry, Tribhuvan University, Pokhara, Nepal. [55]Institute of Evolution, University of Haifa, Haifa, Israel. [56]Scion (New Zealand Forest Research Institute), Christchurch, New Zealand. [57]School of Forestry, University of Canterbury, Christchurch, New Zealand. [58]Institute of Zoology, University of Hamburg, Hamburg, Germany. [59]Faculté des Sciences, Université d'Antananarivo, Antananarivo, Madagascar. [60]Tropical Biodiversity and Social Enterprise, Fort Dauphin, Madagascar. [61]Departamento de Ecologia, Universidade Estadual Paulista, Rio Claro, Brazil. [62]Ecology Group, University Erlangen-Nuremberg, Erlangen, Germany. [63]H. J. Andrews Experimental Forest, Blue River, OR, USA. [64]Environmental and Conservation Sciences, Murdoch University, Melville, Western Australia, Australia. [65]Environmental Futures Research Institute, Griffith University, Nathan, Queensland, Australia. [66]Ashoka Trust for Research in Ecology and the Environment, Bangalore, India. [67] ARC Centre for Forest Value, University of Tasmania, Hobart, Tasmania, Australia. [68]Terrestrial Ecology Research Group, School of Life Sciences, Technical University of Munich, Freising, Germany. [69]EcoBank Team, National Institute of Ecology, Seocheon-gun, Republic of Korea. [70]College of Forestry, Beijing Forestry University, Beijing, China. ✉e-mail: sebastian.seibold@tum.de

# Article

## Methods

### Experimental set-up

We established 55 experimental sites in currently forested areas on six continents and in three major biomes, spanning gradients in mean annual temperature from −1.4 °C to 27.0 °C and mean annual precipitation from 2.90 dm yr$^{-1}$ to 33.86 dm yr$^{-1}$ (Fig. 1a). Sites were located in mature, closed-canopy stands of the dominant zonal forest type and were selected so that structural and compositional characteristics were similar to those of natural forests. To quantify the net effect of insects on wood decomposition, we compared decomposition between uncaged wood accessible to all decomposers (uncaged treatment) and wood in closed cages that excluded insects and other invertebrates (closed-cage treatment) (Extended Data Fig. 1). Cages excluded vertebrate and invertebrate decomposers, but for simplicity, and as insects comprise the functionally most important taxa, we refer to insects throughout the manuscript. To explore the microclimatic effects of caging[44], we added a third treatment of wood in cages with large openings (open-cage treatment) that not only allowed colonization by insects, but also provided similar microclimatic conditions to the closed-cage treatment (Supplementary Information section 1). Analyses across treatments showed that the most robust assessment of the net effect of insects on wood decomposition originated from the uncaged versus closed-cage treatment, as cages had a significant effect on insect colonization, but not on microclimatic conditions, and thus decomposition rates were reduced in the open-cage compared to the uncaged treatment (Supplementary Information section 1 and Extended Data Fig. 2).

Cages measured 40 cm × 40 cm × 60 cm and were made of white polyester mesh with approximately 6,450 mesh per cm². The honeycomb-shaped mesh holes had a width of approximately 0.5 mm. Open cages had four rectangular openings measuring 3 cm × 12 cm at both front sides and four rectangular openings measuring 10 cm × 15 cm at the bottom, representing, in total, 6% of the surface area of the cage. Furthermore, open cages had a total of ten 12-cm slits at the top and long sides. Cages were placed on a stainless-steel mesh (0.5 mm mesh width), which had the same openings as the bottom side of the cages in the open-cage treatment. The top layer of fresh leaf litter was removed before the installation of treatments. The cages and layers of steel mesh were both tightly fixed to the ground using tent pegs, to ensure that all deployed logs had close contact with the soil and to allow water uptake and fungal colonization from the soil. At each site, the three treatments were performed three times—that is, three installations per treatment per site—resulting in a total of nine installations per site (Extended Data Fig. 1). The nine installations were arranged in a matrix of 3 × 3 with a spacing of 2 m between installations, resulting in a total size of approximately 15 m × 15 m. Treatments were assigned randomly to each of the nine locations within a site. The mean spore size and hyphae width of saprotrophic fungal species (mean spore length and width, 8.9 μm and 5.5 μm, respectively[45]; hyphae width, 5–20 μm (refs. [46,47])) are smaller than the mesh width of our cages by an order of magnitude. Rhizomorphs—that is, linear aggregations of several hyphae—can be wider, but during mycelial growth each hypha extends apically rather than the whole rhizomorph[48–50]. Therefore, it is unlikely that the cages hampered fungal colonization. Data loggers recorded air temperature and humidity for the three treatments at nine sites (see Supplementary Information section 1 for details).

### Decomposition measurements

Decomposition was measured as the dry mass loss of unprocessed wood of three of the locally most abundant autochthonous tree species at each study site (Supplementary Table 3-1), as well as for standardized machined wooden dowels. Unprocessed wood of local tree species with the bark retained is more likely to be colonized by local insects and fungi than machined wood without bark[44]. The latter was used to compare the decomposition based on a standardized substrate replicated across all sites. We cut wood of local tree species (around 3 cm in diameter and about 60 cm in length) from either branches or stems of young healthy trees without visible signs of insect or fungal activity. One 5-cm long section was cut from each end of all fresh logs, and the fresh mass of both the cut sections and the resulting 50-cm logs was weighed. The dry mass of all 5-cm sections was measured after drying them at 40 °C until no further mass loss was observed. We calculated the dry mass of the respective 50-cm logs as dry mass$_{50\,cm}$ = (fresh mass$_{50\,cm}$/fresh mass$_{5\,cm}$) × dry mass$_{5\,cm}$. Each installation received three 50-cm long logs of each of the three local tree species and one (closed cage) or two (open cage and uncaged) standardized wooden dowels, giving a total of 96 logs at each site. Standardized dowels (3 cm in diameter, 50 cm in length) were dried machined dowels of *Fagus sylvatica* L. without bark. They were obtained from a single producer in Germany and were then distributed to all sites. Initial dry mass of the dowels was measured directly after drying. All logs and dowels were labelled using numbered plastic tags and assigned randomly to one of the nine installations.

The experiment was established between March 2015 and August 2016 depending on the seasonality of each site. After approximately 1, 2 and 3 years, one of the three installations of each treatment per site was randomly selected and collected to measure wood decomposition. That is, all logs from one uncaged, one closed-cage and one open-cage treatment were collected per site at the same time. We chose this approach because the maximum distance between installations was 6 m and thus within-site variation was expected to be rather low. Moreover, we wanted to ensure that the same number of logs could be sampled per treatment and year and failure of cages over time would have resulted in an unbalanced number of logs per treatment. Owing to the loss of some cages, high decomposition rates at some sites and logistical restrictions, we were not able to maintain the experiment for 3 years at all sites (Supplementary Table 3-1). Litter and soil attached to the wood was removed carefully upon collection, whereas fungal fruit bodies were retained. We assessed insect colonization (presence or absence) for each log based on visible feeding marks, larval tunnels or exit holes for 3,430 (91%) of the analysed logs. The collected logs were dried at 40 °C until the mass remained constant and the dry mass was measured. At sites at which termites were present, logs were burned to account for soil that might have been carried into the wood by these insects[44]. This involved placing one sample at a time onto a steel pan atop a propane burner, and an electrical fan was used to provide aeration and to blow away ash. The residual soil was weighed and its mass subtracted from the dry mass of the wood.

### Statistical analyses of the decomposition experiment

All statistical analyses were performed in R v.4.0.4[51]. For each site, we derived information on average climate conditions from WorldClim (v.2)[52], specifically BIOMOD variables 1 (mean annual temperature) and 12 (mean annual precipitation sum). We modelled relative wood mass loss of local tree species over time using a Gaussian generalized linear mixed model (function glmer in package lme4[53], v.1.1.26) with log link. The dry mass of each individual log at time $t$ served as the response variable and the log-transformed initial dry mass ($t = 0$) was used as an offset term. For each increase of one time unit (1 year), the relative reduction is given by $\exp(\beta)$. Note that the model contained no intercept due to the constraint $\exp(\beta)^0 = 1$. The rate $\exp(\beta)$ was modelled depending on treatment (closed cage versus uncaged) and host type (angiosperm versus gymnosperm), as well as mean annual temperature (°C) and the mean annual precipitation sum (dm yr$^{-1}$). Temperature and precipitation were centred and scaled before modelling, but model coefficients were then back-transformed for ease of interpretation. Reference values for temperature and precipitation were 15 °C and 13 dm yr$^{-1}$, respectively. The model included site-specific random time slopes to deal with clustered observations. On the basis of this model, we computed the fitted annual relative mass loss (as a percentage) for each site considering temperature and precipitation. This was done separately

for angiosperm and gymnosperm wood for all sites where the respective tree species were present. Note that differences in decomposition between tree species could not be tested but were subsumed in the random slope of the site, as most tree species occurred at only a few sites (Supplementary Table 3-1).

To evaluate the potential differences in decomposition rates between the wood of native tree species and standardized wood samples, we estimated the same model for the standardized wooden dowels. Further models were fitted to evaluate the potential microclimatic effects of the cages on decomposition rates and insect colonization. This included one model for the wood decomposition of native tree species for the treatments closed cage versus open cage, and one model comparing the wood decomposition between all three treatment levels (uncaged, closed cage and open cage) using a post hoc test. A binomial generalized linear mixed model was fitted for insect colonization and linear mixed models were fitted for mean daily temperature and mean daily relative humidity. Post hoc tests were applied to these models for comparisons among the three treatments.

## Estimation of global carbon fluxes from deadwood decomposition

To estimate the global carbon flux from deadwood decomposition, we fitted an additive beta regression model (function gam with family betar in package mgcv[54], v.1.8) to the site-specific predicted relative annual mass loss using temperature and precipitation as predictors, separately for angiosperms and gymnosperms. On the basis of the predicted relative annual mass loss for the uncaged treatment, this model was used to predict the total deadwood carbon release globally (that is, attributable to all types of decomposers). To quantify the amount of carbon released from deadwood due to the net effect of insects, we applied the beta regression model to the predicted relative annual mass loss for the closed-cage treatment and calculated it as carbon release$_{uncaged}$ – carbon release$_{closed cage}$.

We applied this model to a spatially explicit global map of carbon stored in deadwood of angiosperms and gymnosperms, which we synthesized from empirical and remote-sensing datasets. We used mean annual temperature and the sum of the mean annual precipitation from WorldClim (v.2)[52] as predictor data. The GlobBiom (http://globbiomass.org) dataset provides high-resolution estimates of forest biomass based on Earth Observation data within the framework of ESA's GlobBiomass project. We used the GlobBiom aboveground biomass layer (that is, the stem, bark and branch compartments) for the reference year 2010, and aggregated information to the base resolution of WorldClim, that is, 5 arcmin (Extended Data Fig. 6a). We extended the aboveground biomass information provided by GlobBiom to total live carbon (including roots) by applying biome-specific root-expansion factors[55] and biome-specific biomass-to-carbon conversion factors between 0.47 and 0.49 (ref. [16]) (Extended Data Fig. 6b). The delineation of forest biomes was taken from FAO[56].

We calculated deadwood carbon stocks at a spatial grain of 5′ by relating deadwood carbon stocks to total live carbon stocks (that is, deadwood carbon fraction). To quantify the regional deadwood carbon fractions, we used previously compiled data[1], which are based on forest inventory data and represent the most comprehensive analysis of global forest carbon stocks available to date. We reanalysed their dataset and amended it with data from the FAO Forest Assessment Report[57] for cases in which values were missing (Extended Data Table 3). Our estimate of global deadwood carbon stocks therefore reflects local differences in forest productivity, mortality and land management. The previously reported values[1] defined deadwood as "all non-living woody biomass not contained in the litter, either standing, lying on the ground, or in the soil" with a diameter of >10 cm. We extended our deadwood carbon pool estimate to include all deadwood with a diameter of >2 cm by applying an expansion factor based on empirical allometric relationships[58]. Our global map of deadwood (Fig. 1a) thus represents the total amount of carbon stored in standing and downed deadwood with a diameter of >2 cm for the reference year 2010.

To differentiate between deadwood of angiosperms and gymnosperms, we used the proportion of broad- and needle-leaved biomass derived from the global land cover product GLCNMO2013[59]. The resolution of GLCNMO2013 is 1/240 degree (that is, each of our 5′ cells contains 400 land cover pixels), and it provides information on 20 land cover classes. We reclassified these to 'broadleaved', 'needle-leaved' and 'mixed forest', and aggregated to 5′ cells for each of the three forest types. The final proportion of each group was calculated assuming that carbon in mixed forests was equally distributed between angiosperms and gymnosperms (Extended Data Fig. 6c).

The experimental sites were chosen to span the global bioclimatic space inhabited by forests. Nonetheless, gaps remained in very cold and dry climatic conditions for both angiosperm and gymnosperm species as well as in very warm and wet climatic conditions for gymnosperm tree species. We constrained the application of our decomposition models to the climate space covered by the experiment to avoid extrapolation beyond our data. Specifically, we defined the bioclimatic space for robust predictions using a convex hull around experimental sites in the temperature–precipitation space (using a buffer of 3° and 3 dm, respectively). Subsequently, climatic conditions outside that convex hull were mapped to the nearest point within the hull in our modelling (Extended Data Fig. 7).

Our statistical model was derived from deadwood samples with a diameter of around 3 cm and thus overestimates annual decomposition rates when applied to the full diameter range of deadwood (Supplementary Information section 2). To address this potential bias, we used a conversion factor relating wood mass loss of fine woody debris (FWD, <10 cm in diameter) to coarse woody debris (CWD, >10 cm). We based our conversion factor on data from 11 peer-reviewed studies reporting data on both CWD and FWD decomposition, covering all major global biomes (Supplementary Table S2-1). As the relationship of the mass loss rate of CWD over the mass loss rate of FWD was robust across different climates, we used its median value (0.53) in our upscaling. An evaluation of the final deadwood decomposition rates used for deriving a global estimate of the carbon flux from deadwood was performed against independent data from 157 previously compiled observations[27]. This evaluation against independent data indicated a good agreement across all major biomes and diameter classes (Extended Data Fig. 4).

Finally, we accounted for the slower carbon release from standing deadwood relative to downed woody debris, particularly in dry regions of the boreal and temperate biome. On the basis of a wood decomposition dataset for standing and downed deadwood across several decay classes for the temperate and boreal biome[60], we estimated the decomposition of standing deadwood to be 33–80% slower compared to lying logs. This is consistent with a detailed analysis for temperate forests in Switzerland[61] that found a slowdown of 42%. In the tropics, however, the decomposition rates of standing trees have the same or sometimes even higher decomposition rates as downed trees[3,62,63]. We assumed a reduction of decomposition rates by 50% for standing deadwood in temperate and boreal forests, and no reduction in the tropical biome in our upscaling. On the basis of large-scale inventories[64–68], we estimated the proportion of standing deadwood of the total deadwood as 25% and 30% for the boreal and temperate biome, respectively.

Our global estimate of the carbon fluxes of deadwood decomposition required a number of analytical steps and assumptions, each of which is associated with uncertainties. These can be classified into uncertainties related to deadwood carbon stocks (data uncertainties), uncertainties related to the statistical modelling of deadwood decomposition (model uncertainties) and uncertainties in the upscaling of the model results to the global scale (scaling uncertainties). To assess the robustness of our estimate, we performed a global sensitivity analysis[69] in which we selected 3–4 indicators for each of these three categories of uncertainty, and estimated their influence on the overall result.

# Article

For each of the ten indicators analysed in total, we selected either a single alternative (for example, the use of the standardized dowels instead of the native species) or an upper and lower bound around the default value based on available data or indicator-specific assumptions (Extended Data Table 2). With regard to data uncertainty, we investigated uncertainties associated with the GlobBiom dataset used as the important data basis here, the deadwood carbon pool estimates[1] and the expansion factors used to derive total biomass from aboveground biomass[55]. Model uncertainties were considered by using alternative models using the 97.5th and 2.5th percentile of parameter values for fixed effects of the original model, an additional model accounting for potential microclimatic effects of cages (that is, using the open-cage instead of the uncaged treatment) and a model based on the results of the standardized dowels (instead of the native tree species). Scaling uncertainties were addressed by analysing alternative expansion factors to include deadwood <10 cm, varying the relationships between the FWD and CWD decay rates, alternative assumptions regarding the proportion and decay rate of standing deadwood, and the treatment of regions outside of the climate envelope covered by our experiment (see Extended Data Table 2 for details). All factor levels of all indicators were allowed to vary simultaneously, resulting in a total of 4,860 estimates for annual deadwood carbon release and the net effects of insects. The relative influence of each indicator on the total uncertainty was derived using an ANOVA, determining the percentage of variance explained by each factor. The contribution at the level of uncertainty categories was derived as the sum of the factors per category. The uncertainty range for the global annual deadwood carbon release estimated from this global sensitivity analysis was ±3.14 Pg C and the net effect of insects varied by ±0.88 Pg C. Data uncertainty was identified as the most important factor (around 40%), but both model and scaling uncertainty were also highly influential, each contributing 25–30% to the overall variation in the results (Extended Data Table 2).

## Data availability

Raw data from the global deadwood experiment, our global map of deadwood carbon and our map of predicted decomposition rates are publicly available from Figshare https://figshare.com/s/ffc39ee0724b11bf450c (https://doi.org/10.6084/m9.figshare.14545992).

## Code availability

An annotated R code including the data needed to reproduce the statistical analyses, global estimates and sensitivity analysis is publicly available from Figshare https://figshare.com/s/ffc39ee0724b11bf450c (https://doi.org/10.6084/m9.figshare.14545992).

44. Ulyshen, M. D. & Wagner, T. L. Quantifying arthropod contributions to wood decay. *Methods Ecol. Evol.* **4**, 345–352 (2013).
45. Bässler, C., Heilmann-Clausen, J., Karasch, P., Brandl, R. & Halbwachs, H. Ectomycorrhizal fungi have larger fruit bodies than saprotrophic fungi. *Fungal Ecol.* **17**, 205–212 (2015).
46. Ryvarden, L. & Gilbertson, R. L. *The Polyporaceae of Europe* (Fungiflora, 1994).
47. Eriksson, J. & Ryvarden, L. *The Corticiaceae of North Europe* Parts 1–8 (Fungiflora, 1987).
48. Boddy, L., Hynes, J., Bebber, D. P. & Fricker, M. D. Saprotrophic cord systems: dispersal mechanisms in space and time. *Mycoscience* **50**, 9–19 (2009).
49. Moore, D. *Fungal Morphogenesis* (Cambridge Univ. Press, 1998).
50. Clemencon, H. *Anatomy of the Hymenomycetes* (Univ. Lausanne, 1997).
51. R Core Team. *R: A language and environment for statistical computing.* (R Foundation for Statistical Computing, 2020).
52. Fick, S. E. & Hijmans, R. J. WorldClim 2: new 1-km spatial resolution climate surfaces for global land areas. *Int. J. Climatol.* **37**, 4302–4315 (2017).
53. Bates, D., Maechler, M., Bolker, B. & Walker, S. Fitting linear mixed-effects models using lme4. *J. Stat. Softw.* **67**, 1–48 (2015).
54. Wood, S. N. *Generalized Additive Models: an Introduction with R* 2nd edn (Chapman and Hall/CRC, 2017).
55. Robinson, D. Implications of a large global root biomass for carbon sink estimates and for soil carbon dynamics. *Proc. R. Soc. B* **274**, 2753–2759 (2007).
56. Food and Agriculture Organization. *Global Ecological Zones for FAO Forest Reporting: 2010 Update, Forest Resource Assessment Working Paper* (Food and Agriculture Organization, 2012).
57. Food and Agriculture Organization. *Global Forest Resources Assessment 2015* (Food and Agriculture Organization, 2016).
58. Christensen, M. et al. Dead wood in European beech (*Fagus sylvatica*) forest reserves. *For. Eco. Man.* **210**, 267–282 (2005).
59. Kobayashi, T. et al. Production of global land cover data – GLCNMO2013. *J. Geogr. Geol.* **9**, 1–15 (2017).
60. Harmon, M. E., Woodall, C. W., Fasth, B., Sexton, J. & Yatkov, M. *Differences between Standing and Downed Dead Tree Wood Density Reduction Factors: A Comparison across Decay Classes and Tree Species* Research Paper NRS-15 (US Department of Agriculture, Forest Service, Northern Research Station, 2011).
61. Hararuk, O., Kurz, W. A. & Didion, M. Dynamics of dead wood decay in Swiss forests. *For. Ecosyst.* **7**, 36 (2020).
62. Gora, E. M., Kneale, R. C., Larjavaara, M. & Muller-Landau, H. C. Dead wood necromass in a moist tropical forest: stocks, fluxes, and spatiotemporal variability. *Ecosystems* **22**, 1189–1205 (2019).
63. Hérault, B. et al. Modeling decay rates of dead wood in a neotropical forest. *Oecologia* **164**, 243–251 (2010).
64. Thünen-Institut für Waldökosysteme. *Der Wald in Deutschland - Ausgewählte Ergebnisse der dritten Bundeswaldinventur* (Bundesministerium für Ernährung und Landwirtschaft, 2014).
65. Puletti, N. et al. A dataset of forest volume deadwood estimates for Europe. *Ann. For. Sci.* **76**, 68 (2019).
66. Richardson, S. J. et al. Deadwood in New Zealand's indigenous forests. *For. Ecol. Manage.* **258**, 2456–2466 (2009).
67. Shorohova, E. & Kapitsa, E. Stand and landscape scale variability in the amount and diversity of coarse woody debris in primeval European boreal forests. *For. Ecol. Manage.* **356**, 273–284 (2015).
68. Szymański, C., Fontana, G. & Sanguinetti, J. Natural and anthropogenic influences on coarse woody debris stocks in Nothofagus–Araucaria forests of northern Patagonia, Argentina. *Austral Ecol.* **42**, 48–60 (2017).
69. Link, K. G. et al. A local and global sensitivity analysis of a mathematical model of coagulation and platelet deposition under flow. *PLoS One* **13**, e0200917 (2018).
70. Saugier, B., Roy, J. & Mooney, H. A. in *Terrestrial Global Productivity* (eds J. Roy, B. Saugier & H. A. Mooney) 543–557 (Academic Press, 2001).

**a** Arrangement of installations



**b** Closed cage
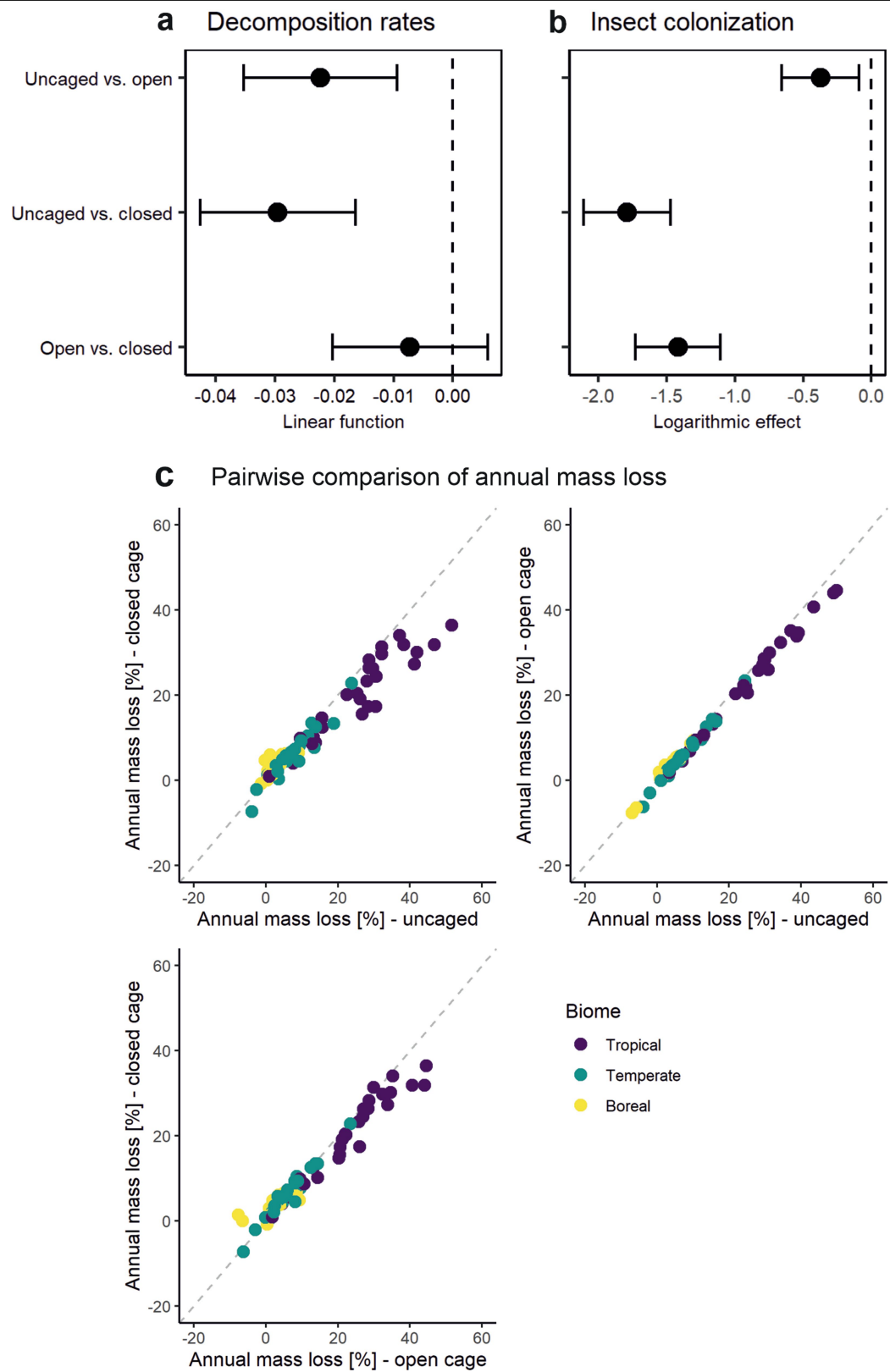


**c** Open cage



**d** Uncaged



**Extended Data Fig. 1 | Arrangement of installations per site and per treatment. a**, Each site received three installations of three treatments randomly assigned to a 3 × 3 grid. **b**–**d**, Treatments included closed cages to exclude insects (**b**), open cages providing similar microclimatic conditions as closed cages but giving access to insects (**c**) and uncaged bundles of logs (**d**). Cages measured 40 cm × 40 cm × 60 cm and were made of white polyester with honeycomb-shaped meshes with a side length of approximately 0.5 mm. Open cages had four rectangular openings measuring 3 cm × 12 cm at both front sides and four rectangular openings measuring 10 cm × 15 cm at the bottom representing in total 6% of the surface area of the cage as well as a total of ten 12-cm slits at the top and long sides. All cages were placed on a stainless-steel mesh (0.5 mm mesh width), which had the same openings as the bottom side of the cages in the open-cage treatment. Photographs show the site in the Bavarian Forest National Park, Germany.
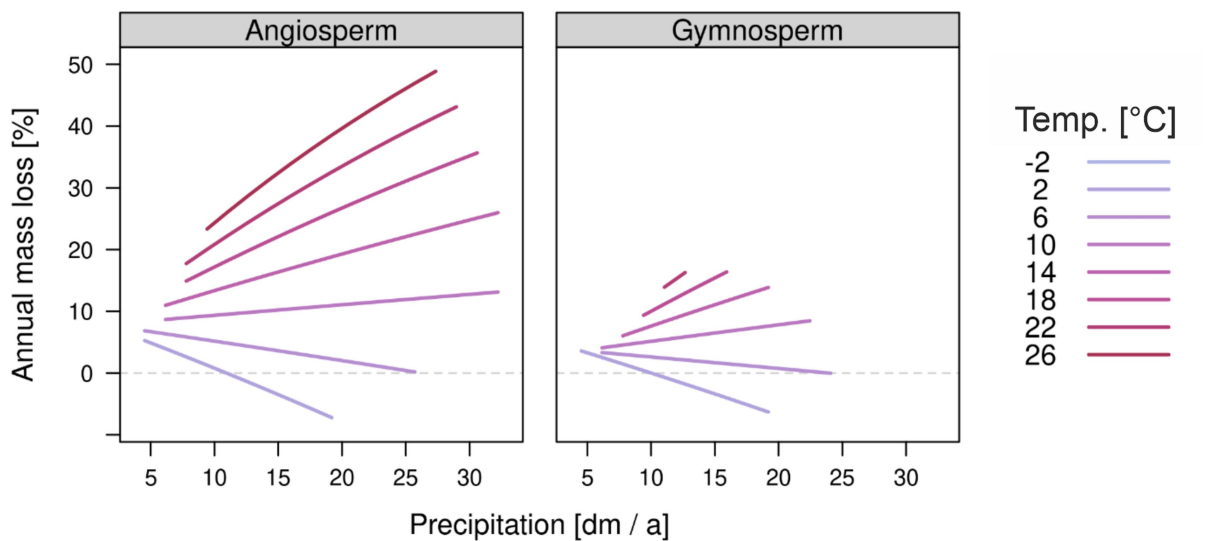
**a** Decomposition rates

**b** Insect colonization

**c** Pairwise comparison of annual mass loss

Biome
- Tropical
- Temperate
- Boreal

**Extended Data Fig. 2** | See next page for caption.

**Extended Data Fig. 2 | Effects of treatments on wood decomposition and insect colonization. a**, **b**, Coefficients and confidence intervals from post hoc tests assessing all three pairwise comparisons between the uncaged, closed-cage and open-cage treatments for annual mass loss (**a**; same structure as the model shown in Table 1 based on 3,578 logs) and insect colonization (**b**; binomial model for insect presence and absence based on 3,430 logs) of wood of native tree species. The 95% confidence intervals that do not intersect the zero line (dashed) indicate significant differences. **c**, Pairwise comparison of fitted annual mass loss (%) between each of the three treatments in the global deadwood decomposition experiment. Points represent the predicted values for angiosperm species at 55 sites and gymnosperm species at 21 sites based on three Gaussian generalized linear mixed log-link models for 3,758 logs with site-specific random effects and temperature, precipitation, treatment (closed cage versus uncaged, open cage versus uncaged and closed cage versus open cage), host division, as well as their interactions, as fixed effects. In **a** and **b**, the largest differences in both response variables were observed between uncaged and closed-cage treatments. Annual mass loss was higher in the uncaged than open-cage treatment and higher in the open-cage than in closed-cage treatment, although the latter was not significant. This indicates that the open cage, despite its openings for insects, has a clearly reduced decomposition rate compared with the uncaged treatment. Insect colonization for the open cage differed significantly from both uncaged and closed-cage treatment, but was more similar to the uncaged than closed-cage treatment. This indicates that open cages were colonized by insects, but not as frequently as the uncaged treatment. Open cages thus excluded parts of the wood-decomposing insect community, which may explain the rather small difference in annual mass loss between closed cages and open cages. These results suggest that the comparison of uncaged wood versus closed cages provides a more reliable estimate of the net effect of insects on wood decomposition than the comparison of closed-cage versus open-cage treatments, which is likely to underestimate the net effect of insects. In **c**, the difference between annual mass loss in closed-cage and both treatments with insect access (uncaged and open cage) increased from boreal to tropical biomes, whereas the difference between uncaged wood and open cages hardly deviated from the 1:1 line. This indicates that the reported mass loss differences between closed-cage and uncaged treatments, as well as the accelerating effect of temperature and precipitation (Table 1), can be attributed to insects and are not an artefact of potential microclimatic effects of the cages (Supplementary Information section 1).

**a** All decomposers



**b** Net insect effect
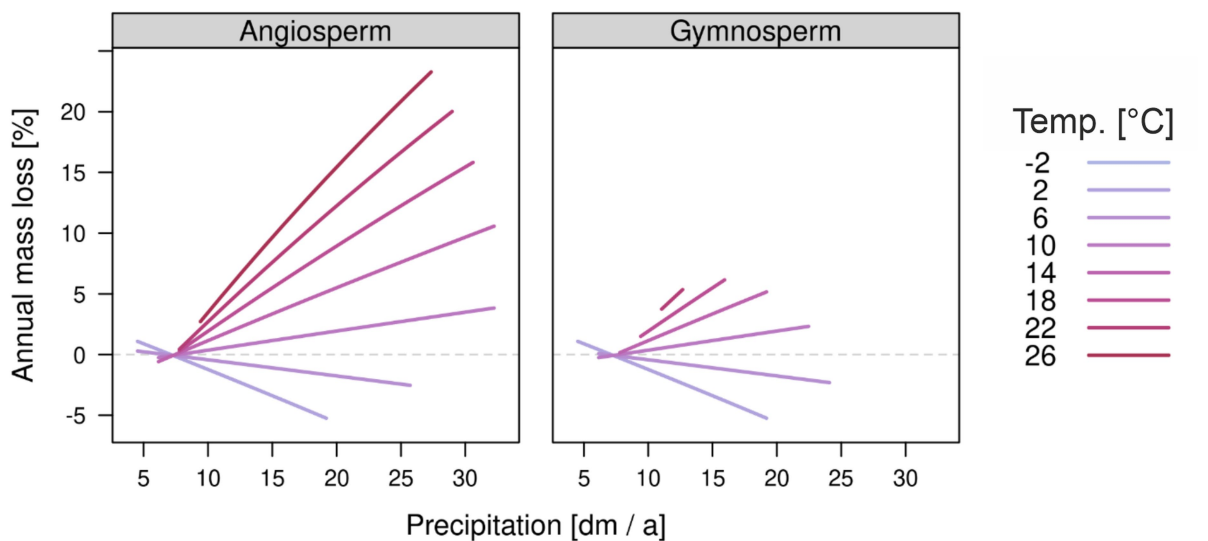


**Extended Data Fig. 3 | Interaction effects of temperature and precipitation on wood decomposition. a, b**, Predictions based on the model presented in Table 1 for annual mass loss of deadwood of native tree species (2,533 logs at 55 sites), considering all possible groups of decomposers (uncaged treatment) (**a**), and annual mass loss attributed to insects (difference in mass loss between uncaged and closed-cage treatments) (**b**), relative to temperature and precipitation. The length of the lines is limited to the gradients in precipitation covered by the sites.
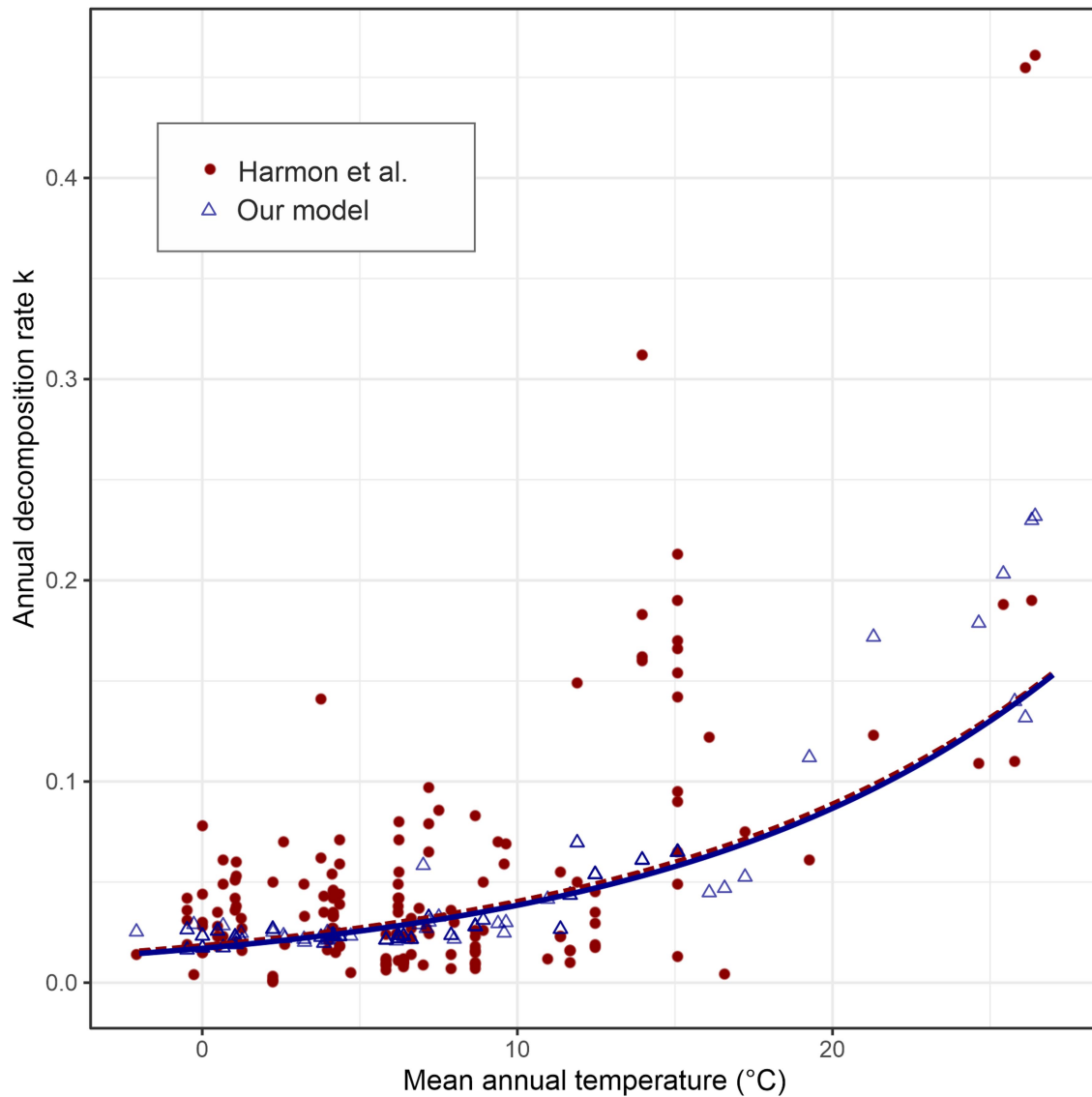
**Extended Data Fig. 4 | Model evaluation against independent data.** Comparison of 157 independent observations of annual deadwood decomposition rates measured for larger diameter wood in previous deadwood surveys[27] (red dots) with the predictions from our model for the same locations (blue triangles). Lines indicate the relationship between the decomposition rate and mean annual temperature from Harmon et al.[27] (red dashed line; $k = 0.0184e^{0.0787 \times temperature}$) and for our model (blue line; $k = 0.0171e^{0.0812 \times temperature}$). Good correspondence of both curves indicates that our models of global carbon release from deadwood provide robust estimates despite being based on experimental deadwood with a diameter of around 3 cm (for detailed discussion, see Supplementary Information section 1).

## a Annual deadwood carbon release
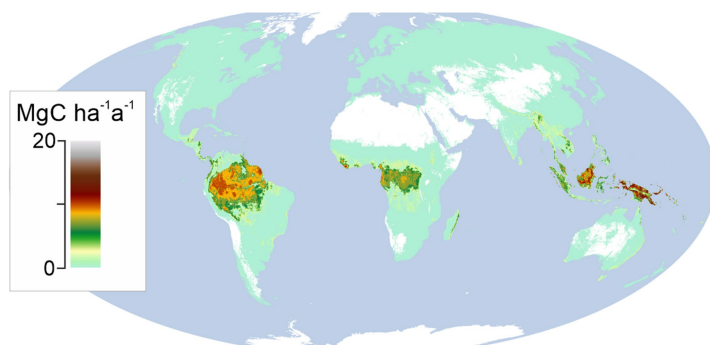
## b Net insect effect
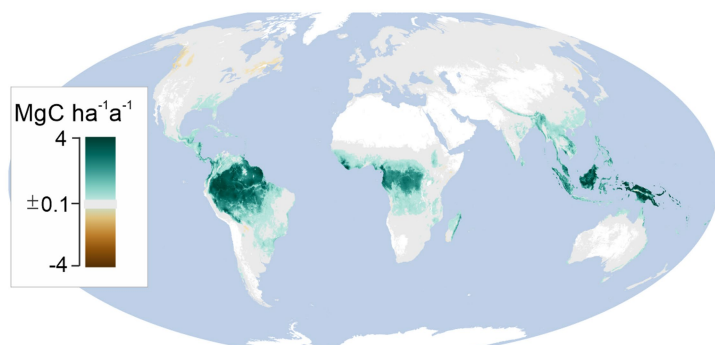
## c Latitudinal distribution
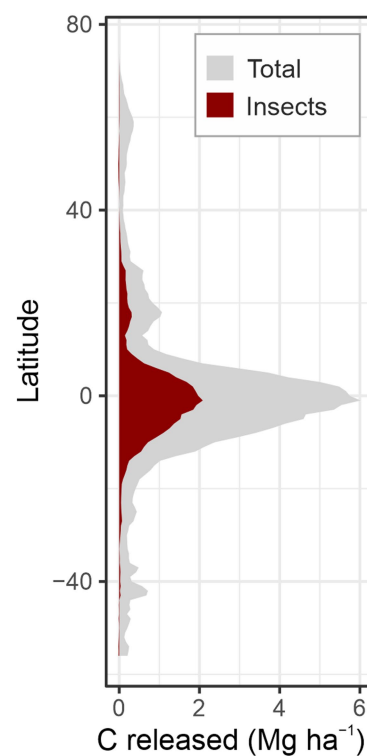


**Extended Data Fig. 5 | Global deadwood carbon fluxes. a, b,** Total annual release of deadwood carbon from decomposition including all decomposers (**a**) and annual release of deadwood carbon due to the net effect of insects (**b**). Light grey areas indicate values of ±0.1 Mg C ha$^{-1}$ yr$^{-1}$ and white areas are non-forest systems. **c,** Latitudinal distribution of global deadwood carbon fluxes per hectare.
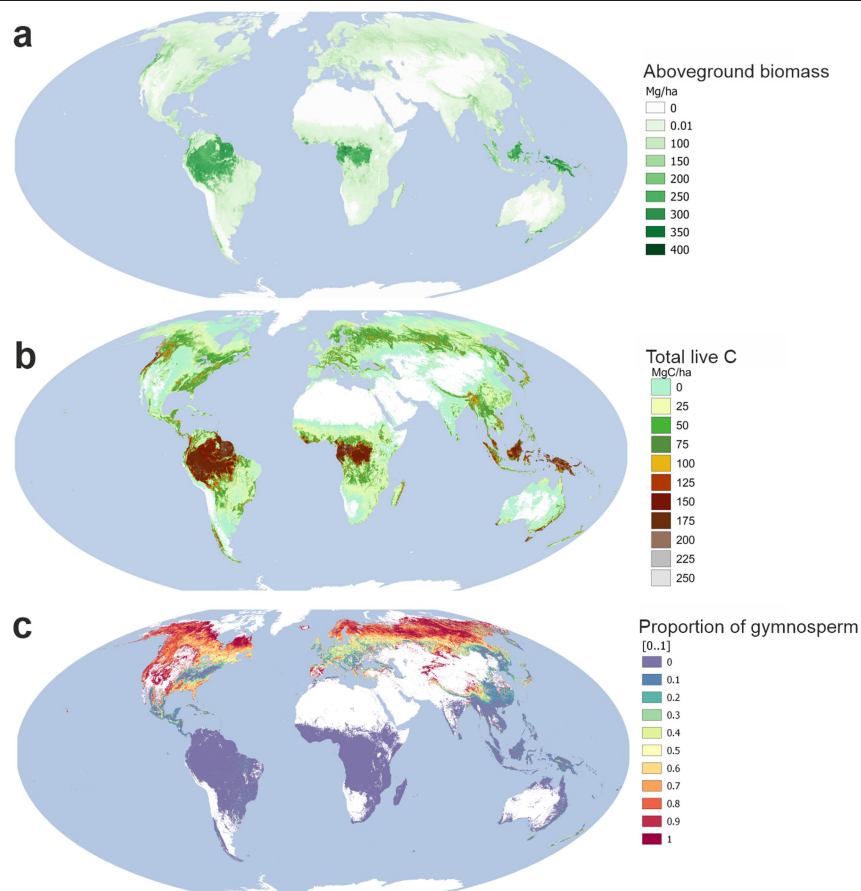
**Extended Data Fig. 6 | Processing steps for the global deadwood carbon map. a**, Aboveground forest biomass (Mg ha$^{-1}$) aggregated to 5′ from the GlobBiom dataset. **b**, Total live carbon (Mg ha$^{-1}$) by extending **a** with root biomass[55] and conversion to carbon. **c**, Proportion of gymnosperm forests derived from the GLCNMO2013[59] dataset. The proportion of angiosperm cover is 1 − gymnosperm cover. White indicates non-forested area.

**a** Angiosperm
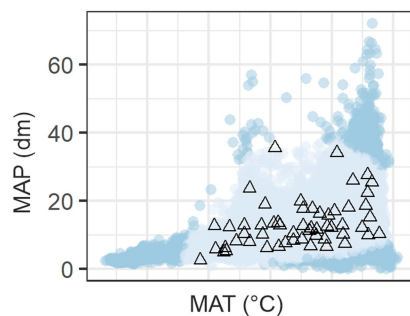


**b** Gymnosperm
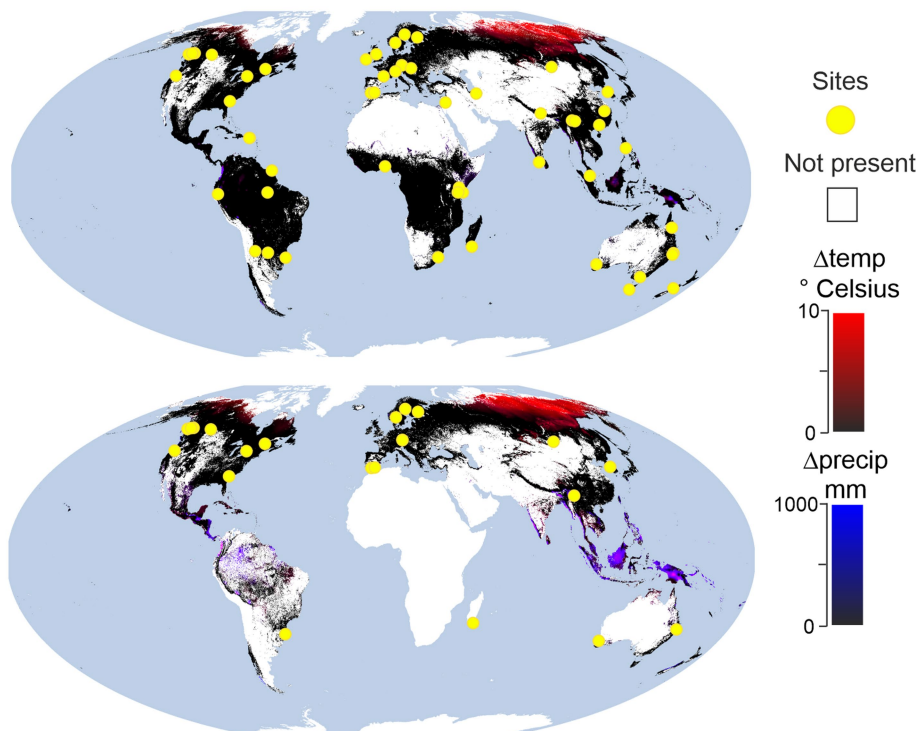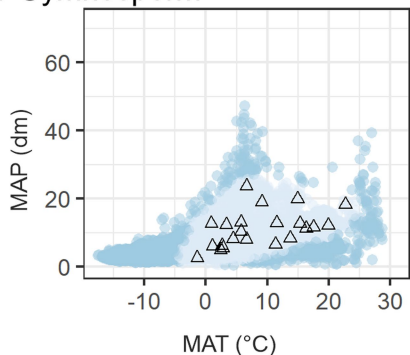


**Extended Data Fig. 7 | Bioclimatic space for robust predictions. a, b,** Climate conditions outside of the range of prediction models for angiosperm (**a**) and gymnosperm (**b**) species in climate space (left) and mapped (right). Left, dark blue points are outside of the range defined by a convex hull around the experimental sites (black triangles). Right, the colours on the maps indicate the absolute difference between the local climate and the climate used for prediction for temperature (red colour channel) and precipitation (blue colour channel) with black indicating no difference. White areas indicate that no gymnosperm or angiosperm forest, respectively, occurs there. Experimental sites are indicated by yellow dots. Temperatures outside of the range are mainly located in northeastern Siberia and northern Canada, whereas offsets in precipitation are stronger for gymnosperms in southeastern Asia, Indonesia and in the Amazon region. The land surface area not covered by our experimental data is 23.5% for gymnosperms and 17.7% for angiosperms, representing together 13.2% of the carbon stored in deadwood. These areas were included in our upscaling by mapping them to the nearest point at the convex hull in climate space.

**Extended Data Table 1 | Supporting analyses of drivers of wood decomposition**

| Predictor | Estimate * 10³ | Std.Error * 10³ | z-value | p-value | Relative effect and 95% confidence interval |
|---|---|---|---|---|---|
| **a)    Standardized dowels** | | | | | |
| Temperature (in °C - 15) | -17.918 | 3.922 | -4.569 | <0.001 | 0.982 (0.975 - 0.990) |
| Precipitation (in dm a⁻¹ -13) | -6.195 | 4.269 | -1.451 | 0.147 | 0.994 (0.986 - 1.002) |
| Treatment: uncaged vs. closed | -46.570 | 11.450 | -4.067 | <0.001 | 0.954 (0.933 - 0.976) |
| Temperature*precipitation | -1.597 | 0.502 | -3.182 | 0.001 | 0.998 (0.997 - 0.999) |
| Temperature*treatment | -5.024 | 1.598 | -3.144 | 0.002 | 0.995 (0.992 - 0.998) |
| Precipitation*treatment | -3.595 | 1.945 | -1.849 | 0.065 | 0.996 (0.993 — 1.000) |
| Temperature*precipitation*treatment | -0.637 | 0.275 | -2.320 | 0.020 | 0.999 (0.999 — 1.000) |
| **b)    Native tree species** | | | | | |
| Temperature (in °C - 15) | -9.906 | 2.936 | -3.374 | 0.001 | 0.990 (0.984 - 0.996) |
| Precipitation (in dm a⁻¹ -13) | -4.343 | 3.268 | -1.329 | 0.184 | 0.996 (0.989 - 1.002) |
| Host: angiosperm | -147.400 | 22.040 | -6.688 | <0.001 | 0.863 (0.826 - 0.901) |
| Host: gymnosperm | -66.540 | 24.460 | -2.720 | 0.007 | 0.936 (0.892 - 0.982) |
| Treatment: open vs. closed | -6.363 | 5.138 | -1.238 | 0.216 | 0.994 (0.984 - 1.004) |
| Temperature*precipitation | -0.614 | 0.388 | -1.581 | 0.114 | 0.999 (0.999 — 1.000) |
| Temperature*host | 5.653 | 1.236 | 4.572 | <0.001 | 1.006 (1.003 - 1.008) |
| Precipitation*host | -0.251 | 3.189 | -0.079 | 0.937 | 1.000 (0.994 - 1.006) |
| Temperature*treatment | -1.590 | 0.674 | -2.358 | 0.018 | 0.998 (0.997 — 1.000) |
| Precipitation*treatment | -3.027 | 0.809 | -3.742 | <0.001 | 0.997 (0.995 - 0.999) |
| Temperature*precipitation*host | 0.090 | 0.293 | 0.308 | 0.758 | 1.000 (1.000 - 1.001) |
| Temperature*precipitation*treatment | -0.486 | 0.102 | -4.759 | <0.001 | 1.000 (0.999 — 1.000) |

a, b, Results from Gaussian generalized linear mixed log-link models of the relative annual mass loss of standardized wooden dowels comparing the uncaged versus closed-cage treatments (415 logs from 55 sites) (a) and wood of native tree species comparing the open-cage and closed-cage treatments (2,522 logs from 55 sites) (b). Models include the mean annual temperature and the mean annual precipitation, which were both centred and scaled, the host tree type (angiosperm versus gymnosperm; in b only) and treatment, as well as their two- and three-way interactions, as fixed effects and site as the random effect. Estimates and standard errors (std. error) for temperature and precipitation are transformed back to °C and decimetres per year (dm yr⁻¹), respectively. The main effects of each variable are interpretable when the remaining variables are fixed at their reference value (15°C and 13 dm yr⁻¹).

**Extended Data Table 2 | Uncertainty in global carbon fluxes from the decomposition of deadwood, determined in a global sensitivity analysis**

| Source of uncertainty | Value range | Description | Annual deadwood carbon release | | Net effect of insects | |
|---|---|---|---|---|---|---|
| | | | Uncertainty Pg | Contribution to uncertainty (%) | Uncertainty Pg | Contribution to uncertainty (%) |
| **Total uncertainty** | | | ±3.22 | | ±0.88 | |
| **Data uncertainty** | | | ±2.03 | 42.64 | ±0.59 | 38.22 |
| Above-ground biomass | ± 10% | Based on regional assessment against plot data for the tropical biome (GlobBiomass D17 Validation report) | ±0.99 | 10.82 | ±0.29 | 9.73 |
| Proportion deadwood / total C stock | ± 15% | Twice the uncertainty of global stock estimates reported by Pan et al. [1] | ±1.48 | 24.35 | ±0.43 | 21.89 |
| Proportion of root C to total C | +10% | Based on an alternative estimate of Robinson et al.[55] (assumption iii, less conservative compared to the value given by Saugier et al.[70]) | ±0.90 | 7.47 | ±0.26 | 6.60 |
| **Model uncertainty** | | | ±1.88 | 28.50 | ±0.56 | 33.07 |
| Model CI | ±CI | Lower and upper bounds of model predictions with CI of fixed effects (lower and upper bounds) | ±1.86 | 19.52 | ±0.16 | 2.06 |
| Open:closed caged (microclimate effect) | Yes/No | Model based on data from the "open" instead of "uncaged" treatment (microclimate effect) | ±0.70 | 2.27 | ±0.72 | 30.98 |
| Standardized dowel | Yes/No | Model based on standardized dowels instead of native trees (tree species effect) | ±1.03 | 6.71 | ±0.17 | 0.03 |
| **Scaling uncertainty** | | | ±1.49 | 26.44 | ±0.43 | 26.25 |
| Expansion FWD | ± 25% | Expansion factor to estimate deadwood pools >2cm from pools >10cm. We assumed high uncertainty as the relationship used[58] is based on only one forest type | ±0.43 | 2.05 | ±0.12 | 1.85 |
| Standing deadwood | slower/ faster | Fraction of standing deadwood, and assumptions for decay rate of SWD. Boreal: slower: SWD=30% of total deadwood, no decay; faster: SWD=20% of total deadwood, 50% slower. Temperate: slower: SWD=40%, 50% slower, faster: SWD=20%, decay as fast as DWD | ±0.07 | 0.08 | ±0.07 | 0.00 |
| Rate FWD:CWD | ± 15% | The lower value assumes that the empirically determined FWD:CWD decay ratio from tropical forests[3] is applicable across the entire globe, while the upper value assumes an FWD:CWD decay ratio at the 90th percentile of the available data. | ±1.48 | 24.35 | ±0.43 | 21.89 |
| Climate envelope | Reduced / expanded | Reduced/expanded definition of the convex hull that limits the extrapolation to climatic conditions not covered by our experiment. Reduced: limit the convex hull to 0.5° and 0.5 dm around observed conditions, expanded: no limit to extrapolation | ±0.11 | 0.04 | ±0.02 | 2.51 |

Important factors per uncertainty category were selected and allowed to vary simultaneously, resulting in a total of 4,860 analysed combinations. The uncertainty of total annual deadwood carbon released and of the net effect of insects was calculated as the s.d. over all combinations for each factor, with all other factors fixed to their default value. Similarly, the uncertainty per category was calculated over all combinations within a category, with all factors from other categories fixed to the default value. The relative contribution of each factor to overall uncertainty was derived using an ANOVA, estimating the percentage of variance explained for each factor. The contribution at the level of uncertainty categories is the sum of the respective factors in each category. Descriptions are based on refs. [1,3,55,58,70] as indicated. DWD, downed woody debris; SWD, standing woody debris.

**Extended Data Table 3 | Comparison of global carbon stock estimates and results for each biome**

**a**

| | Total live carbon Pan et al.[1] | Total live carbon this study | Deadwood carbon Pan et al.[1] | Deadwood carbon this study |
|---|---|---|---|---|
| **Boreal** | 53.9 | 60.2 (+11.7%) | 16.1 | 17.8 (+10.5%) |
| **Temperate** | 46.6 | 53.5 (+14.8%) | 3.3 | 9.3 (+182.2%) |
| **Tropical** | 262.1 | 272.7 (+4.0%) | 53.6 | 49.4 (-7.9%) |
| **World** | 362.6 | 386.5 (+6.6%) | 73.0 | 76.5 (+4.8%) |

**b**

| | Annual deadwood carbon release | Net effect of insects | Deadwool carbon residence time |
|---|---|---|---|
| **Boreal** | 0.44 | 0.003 | 40.0 |
| **Temperate** | 0.28 | -0.009 | 33.3 |
| **Tropical** | 10.22 | 3.18 | 4.8 |
| **World** | 10.94 | 3.17 | 7.0 |

**a**, Global estimates of total live carbon and carbon in deadwood (>10 cm) from Pan et al.[1] compared with estimates obtained in this study (>2 cm) in Pg. Numbers in parentheses indicate the difference as a percentage. Note that Pan et al.[1] defined biomes at the country level whereas we define biomes here using the FAO Global Ecological Zones. Differences between these biome definitions are especially marked for the temperate biome, as temperate parts of Russia and Canada are included in the boreal biome in Pan et al.[1], whereas we divide Russia and Canada into boreal and temperate regions in our study. Furthermore, missing and unrealistic deadwood carbon stocks for a number of areas (specifically Japan, South Korea, China, Australia and Alaska) in Pan et al.[1] were complemented with data from the FAO Forest Assessment Report[57] in this study, which contributes to higher deadwood carbon estimates relative to Pan et al.[1]. **b**, Annual deadwood carbon release and net insect effect per biome (in Pg) and calculated residence time of deadwood carbon (years).